NeuroImage: Clinical 16 (2017) 557–563

Contents lists available at ScienceDirect

NeuroImage: Clinical

journal homepage: www.elsevier.com/locate/ynicl

Evaluation of striatonigral connectivity using probabilistic tractography in Parkinson's disease

Frances Theisen[a,b], Rebecca Leda[a,b], Vincent Pozorski[a,b], Jennifer M. Oh[a,c], Nagesh Adluru[e], Rachel Wong[a,b], Ozioma Okonkwo[a,c], Douglas C. Dean III[e], Barbara B. Bendlin[a,c], Sterling C. Johnson[a,c], Andrew L. Alexander[d,e,f], Catherine L. Gallagher[a,b,c,*]

[a] William S. Middleton Memorial Veterans Hospital, Madison, WI, USA
[b] Department of Neurology, University of Wisconsin Madison, Madison, WI, USA
[c] Wisconsin Alzheimer's Disease Research Center, University of Wisconsin School of Medicine and Public Health, Madison, WI, USA
[d] Department of Medical Physics, University of Wisconsin School of Medicine and Public Health, Madison, WI, USA
[e] Waisman Laboratory for Brain Imaging and Behavior, Waisman Center, University of Wisconsin – Madison, Madison, WI, USA
[f] Department of Psychiatry, University of Wisconsin School of Medicine and Public Health, Madison, WI, USA

ARTICLE INFO

Keywords:
Aged brain/metabolism/*pathology
Diffusion tensor imaging/*methods
Parkinson disease/classification/*pathology
Humans
Severity of illness index

ABSTRACT

The cardinal movement abnormalities of Parkinson's disease (PD), including tremor, muscle rigidity, and reduced speed and frequency of movements, are caused by degeneration of dopaminergic neurons in the substantia nigra that project to the putamen, compromising information flow through frontal-subcortical circuits. Typically, the nigrostriatal pathway is more severely affected on the side of the brain opposite (contralateral) to the side of the body that manifests initial symptoms. Several studies have suggested that PD is also associated with changes in white matter microstructural integrity. The goal of the present study was to further develop methods for measuring striatonigral connectivity differences between PD patients and age-matched controls using diffusion weighted magnetic resonance imaging (MRI).

In this cross-sectional study, 40 PD patients and 44 controls underwent diffusion weighted imaging (DWI) using a 40-direction MRI sequence as well as an optimized 60-direction sequence with overlapping slices. Regions of interest (ROIs) encompassing the putamen and substantia nigra were hand drawn in the space of the 40-direction data using high-contrast structural images and then coregistered to the 60-direction data. Probabilistic tractography was performed in the native space of each dataset by seeding the putamen ROI with an ipsilateral substantia nigra classification target. The effect of disease group (PD versus control) on mean putamen-SN connection probability and streamline density were then analyzed using generalized linear models controlling for age, gender, education, as well as seed and target region characteristics.

Mean putamen-SN streamline density was lower in PD on both sides of the brain and in both 40- and 60-direction data. The optimized sequence provided a greater separation between PD and control means; however, individual values overlapped between groups. The 60-direction data also yielded mean connection probability values either trending (ipsilateral) or significantly (contralateral) lower in the PD group. There were minor between-group differences in average diffusion measures within the substantia nigra ROIs that did not affect the results of the GLM analyses when included as covariates. Based on these results, we conclude that mean striatonigral structural connectivity differs between PD and control groups and that use of an optimized 60-direction DWI sequence with overlapping slices increases the sensitivity of the technique to putative disease-related differences. However, overlap in individual values between disease groups limits its use as a classifier.

Abbreviations: ADRC, Alzheimer's Disease Research Center; AFNI, Analysis of Functional NeuroImages; BET, brain extraction tool; DWI, diffusion-weighted imaging; FA, fractional anisotropy; FLAIR, fluid attenuated inversion recovery; FOV, field of view; FSL, Oxford Centre for Functional MRI of the Brain Software Library; GE, general electric; HY, Hoehn and Yahr; ICC, interclass correlation coefficient; IRB, institutional review board; LMPD, longitudinal MRI biomarkers in Parkinson's disease study; MD, mean diffusivity; MRI, magnetic resonance imaging; PD, Parkinson's disease; PET, Positron Emission Tomography; RD, radial diffusivity; ROI, region of interest; SD, standard deviation; SN, substantia nigra; SNR, signal to noise ratio; SPECT, single photon emission tomography; SPM, Statistical Parametric Mapping software; TE, echo time; TI, inversion time; TR, repetition time; TFCE, threshold-free cluster enhancement; UPDRS, Unified Parkinson Disease Rating Scale; VA, Veterans Affairs

* Corresponding author at: 7211 MFCB, 1685 Highland Ave., Madison, WI 53705-2281, USA.
E-mail address: gallagher@neurology.wisc.edu (C.L. Gallagher).

http://dx.doi.org/10.1016/j.nicl.2017.09.009
Received 8 March 2017; Received in revised form 7 July 2017; Accepted 6 September 2017
Available online 09 September 2017

1. Introduction

Parkinson's disease (PD) is a common age-related neurodegenerative disease that is diagnosed on the basis of motor symptoms of resting tremor, bradykinesia, and rigidity, which are frequently asymmetrical at symptom onset. These motor symptoms are related to degeneration of dopaminergic neurons in the substantia nigra (SN) pars compacta that project to the striatum (caudate nucleus and putamen; Braak et al., 2003). Mammalian studies have shown that nigrostriatal projections arise from the ventral portion of the SN and ventral tegmental area, forming a broad bundle of axons that run through the brainstem tegmentum ventromedial to the red nucleus, the diencephalic prerubral field, and the dorsal and lateral hypothalamic area as well as medial portion of the internal capsule to distribute throughout the striatum (Moore and Bloom, 1978). Afferent connections from striatum to SN terminate mainly in the pars reticulata with a few fibers reaching the pars compacta (Parent, 1990).

Thus far, restorative treatments for PD, especially transplantation of fetal dopaminergic precursors into the striatum, have produced suboptimal results, in part due to lack of physiologic integration of the transplanted neurons into brain networks (Freed et al., 2001; Goren et al., 2005). As new treatments enter clinical trials, there will be a need for accurate biomarkers not only of dopamine cell survival but also of their function and connectivity (Palfi et al., 2002). Currently, the nigrostriatal pathway is best evaluated in vivo using Positron Emission Tomography (PET) or Single Photon Emission Tomography (SPECT) radiotracers that target dopamine metabolism, binding, or reuptake. These imaging methods are somewhat susceptible to floor effects (Karimi et al., 2013) and cannot evaluate the integration of dopamine-producing transplants into neural networks. Thus, the development of new non-invasive ways to measure striatonigral connectivity is highly desirable, if technically difficult. Such technical difficulties include limited spatial resolution of current imaging methods relative to the size of the nigrostriatal pathway, location of the pathway within the brainstem, which is susceptible to motion and misregistration errors, and abundance of large adjacent white matter bundles such as the corticospinal tract.

For this study, we used a hypothesis-driven approach to quantify structural connections between the putamen and SN from diffusion weighted imaging (DWI) data using probabilistic tractography. Unlike deterministic tractography, in which streamlines or “tracks” follow a single estimated orientation of the primary diffusion direction, probabilistic tractography also models error in the diffusion estimates. As a result, the directional orientation of vectors modeled probabilistically varies between samples, so not all samples will result in a streamline that reaches the target region. In gray matter regions where the isotropic (equal in all directions) component of diffusion is large and the anisotropic (directional) component small, there is greater variability in directional estimates such that few streamlines are generated. Nonetheless, probabilistic tractography is robust to noise since tracks that propagate in non-anatomic directions soon “die out” due to random orientations of fiber orientation estimates in the adjacent voxels (Behrens et al., 2003b), and less susceptible to signal drop out in areas of crossing fibers (Behrens et al., 2007). For the present study we compared results derived from two diffusion weighted imaging (DWI) sequences, a 40-direction sequence that has been used by our lab in other studies of aging and neurodegeneration (Ly et al., 2016), as well a 60-direction sequence with higher spatial and angular resolution, designed specifically for this project. The rationale for using two DWI sequences was to evaluate replicability of the technique, as well as to see if results from the optimized sequence would better separate PD and control groups. We hypothesized that PD patients would have lower structural connectivity between putamen and SN than their healthy counterparts.

2. Methods

2.1. Study participants

Forty Parkinson's disease (PD) patients and 44 age- and gender-matched controls were recruited as part of the VA-sponsored “Longitudinal MRI biomarkers in Parkinson's disease” (LMPD) study. Participants were recruited from local neurology clinics, through the University of Wisconsin Alzheimer's Disease Research Center (ADRC) recruitment database, and from local support groups. To be enrolled, PD participants had to meet UK Brain Bank criteria for Parkinson's disease (Hughes et al., 1992), be at least 45 years of age at symptom onset (to exclude most genetic causes of Parkinson's disease; Lucking et al., 2000), and be free of significant cognitive impairment (Mini Mental State Examination score of 27–30; Folstein et al., 1975). Exclusion criteria included clinically suspected “atypical” Parkinsonian syndrome, dementia, other central nervous system disease (multiple sclerosis, stroke, encephalitis), major psychiatric or medical disease, family history of PD in two or more first-degree relatives, and inability to hold anti-Parkinson medications for 12–18 h. The University of Wisconsin-Madison's institutional review board and the W.S. Middleton V.A. R. & D. committee approved this study and all participants provided written informed consent prior to participation.

2.2. Procedures

Study procedures included a structured interview to determine the nature and duration of motor, sensory, autonomic, and cognitive symptoms potentially related to PD, Unified Parkinson's Disease Rating Scale (UPDRS; Fahn and Elton, 1987) scoring by a movement disorders neurologist (C.G.), neuropsychological testing, and brain imaging. PD participants were off anti-Parkinson medications for 12–18 h prior to and during study procedures.

2.2.1. Image acquisition

Participants were scanned on a GE 750 Discovery 3T MRI system (GE Healthcare, Waukesha, WI) with an 8-channel phased array head coil. Two structural magnetic resonance imaging (MRI) sequences were acquired to define regions of interest for tractography. A high-resolution 3D Brain Volume Imaging (BRAVO) T1-weighted inversion-prepared sequence of repetition time (TR) = 8.2 ms, echo time (TE) = 3.2 ms, inversion time (TI) = 450 ms, flip angle = 12 degrees, field of view (FOV) = 256 mm, matrix = 256 × 256, slice thickness = 1.0 mm was acquired to define the putamen for precise hand tracing. A fluid-attenuated inversion recovery (FLAIR) sequence of TR = 6000 ms, TE = 124 ms, TI = 1867 ms, flip angle = 90 degrees, FOV = 256 mm, matrix = 256 × 256, slice thickness = 2.0 mm was acquired to provide contrast for defining the SN. DWI data were acquired with a diffusion-weighted echo planar imaging sequence with ASSET parallel imaging (undersampling R = 2 in the phase encoding direction), and higher order shimming prior to the acquisition of each sequence. For this project, we used two DWI protocols, a 40-direction sequence that has been used in prior ADRC studies (Ly et al., 2016), as well as an optimized 60-direction sequence with overlapping slices. The 40-direction (b = 1300 s/mm^2) diffusion weighted imaging (DWI) protocol included 52 contiguous, 2.9 mm thick axial slices of TR = 8000 ms, TE = 86.3 ms, FOV = 240 mm, matrix = 96 × 96 to yield 2.5 × 2.5 × 2.9 mm^3 resolution which was interpolated in-plane on the scanner to 0.94 mm voxels. The 60-direction (b = 1300 s/mm^2) DWI protocol included 55 overlapping 3.0 mm thick axial slices spaced every 1.5 mm, TR = 6500 ms, TE = 68.9 ms, FOV = 192 mm, matrix = 128 × 128 to yield 1.5 × 1.5 × 3.0 mm^3 resolution, which is upsampled to 0.75 × 0.75 × 1.5 mm voxels on the scanner. The thicker overlapping slices provided both higher signal to noise ratio (SNR) and finer spatial sampling than typical DWI sequences. Each DWI protocol included eight non-diffusion weighted volumes (b = 0). The

40-direction sequence covered the entire cerebrum, while the 60-direction sequence covered the superior extent of the lateral ventricles to base of the brainstem.

2.2.2. Image preprocessing

DWI data were processed using the diffusion toolbox (FDT) of Functional Magnetic Resonance Imaging of the Brain (FMRIB) Software Library (FSL), version 5 (Jenkinson et al., 2012). Automated inspection of the image series using DTIprep (Oguz et al., 2014) showed that the number of volumes that failed quality measures (in most cases due to between-frame motion) was highly similar between PD and control groups (mean of flagged volumes = 0.8 for the control group and 1.0 for the PD group; 2-tailed P = 0.42). Head motion and image distortions (stretches and shears) due to eddy currents were corrected with affine transformation in FDT. A binary brain mask was created from the B0 image using Brain Extraction Tool (BET; Smith, 2002) with fractional intensity set to 0.1. Subsequently, a diffusion tensor model was fit at each voxel to the 4D DWI data series (with additional inputs of the binary brain mask and gradient table) using DTIFit (Behrens et al., 2003b). The outputs from this process included fractional anisotropy (FA) and mean diffusivity (MD) maps as well as 1st-3rd eigenvector and eigenvalue maps, which were visually inspected as a quality control measure. Diffusion parameters were then modeled using FSL's Bayesian Estimation of Diffusion Parameters Obtained using Sampling Techniques and modeling crossing fibers (BEDPOSTX). BEDPOSTX models diffusion signal as ball (isotropic) and stick (anisotropic) components to generate a distribution of likely fiber orientations within each voxel as well as an estimate of the uncertainty on these orientations (https://fsl.fmrib.ox.ac.uk/fslcourse/lectures/fdt2.pdf). This technique uses Markov Chain Monte Carlo sampling to build posterior distributions on diffusion parameters at each voxel that can then be repeatedly sampled to allow voxel-to-voxel propegation of streamlines until stopping criteria are met (Behrens et al., 2007; Behrens et al., 2003b).

2.2.3. Region of interest selection

Regions of interest (ROIs) encompassing the putamen and substantia nigra were hand drawn in Analysis of Functional NeuroImages (AFNI; https://afni.nimh.nih.gov/afni) by two researchers (R.L., V.P.) who were blind to subject's diagnosis, and whose inter-rater reliability (ICC) was 0.99 based on ROI volume. We did not differentiate SN pars compacta from pars reticulata as they were not resolvable on the FLAIR images. ROIs were drawn on T1 and FLAIR images in register with each subject's FA map generated from the 40-direction sequence in native DWI space (see Fig. 1, ROI method). On T1-weighted images, borders of the putamen were defined medially by the internal capsule and lateral medullary lamina/globus pallidus and laterally by the external capsule. Tracing was discontinued one slice below the anterior commissure. On FLAIR images, the substantia nigra was defined as all low signal in the brainstem between the level of the red nucleus and the superior cerebellar peduncle. After being drawn with reference to the T1 and FLAIR images, the ROIs were visually inspected against the FA map and minor manual edits made to exclude voxels that extended into surrounding white matter. Final ROI volumes (in number of voxels) were compared across hemispheres; cases in which inter-hemispheric volumes differed by > 10% for substantia nigra and > 20% for putamen were inspected and redrawn as necessary. Finalized ROIs that had been drawn with reference to the 40-direction data were then coregistered to the 60-direction data by first coregistering equivalent parameter maps by trilinear interpolation in FMRIB's Linear Image Registration Tool (FLIRT) (Greve and Fischl, 2009; Jenkinson et al., 2002; Jenkinson and Smith, 2001) and then applying the resulting transforms to the ROIs in 40-direction space to bring them into 60-direction space. Finally, ROIs in register with 40- and 60-direction DWI data were simultaneously visually inspected and minor manual edits performed to improve coverage of the putamen and SN. Mean FA and MD values within the finalized putamen and SN ROIs were then extracted from the aligned 40- and 60-direction DWI data using FSLmaths.

2.2.4. Tractography

Probabilistic tractography was performed using FSL's Probtrackx 2.0. As described above, care was taken not to resample either 40- and 60-direction diffusion data prior to tractography. For each subject, brain hemisphere, and DWI sequence, each voxel in the putamen was seeded with 5000 streamline samples that migrated according to local probability density functions – those that contacted the SN were retained as estimates of putamen-SN structural connectivity (Behrens et al., 2007; Behrens et al., 2003b). Since DTI tractography models connections between two anatomical ROIs without distinguishing afferent from efferent connections, we refer to the resulting tracks as “striatonigral”. We used Probtrackx 2.0 default settings of 5000 samples/voxel, step length (0.5 mm), curvature threshold (0.2), and “loopcheck” to exclude tracks that double back on themselves. The “classification target” option, in which the putamen ROI was the seed mask and the ipsilateral SN the classification target, was employed. After tractography, for each voxel in the putamen seed ROI, 0 (blue in Fig. 2) or a number (1–200 as orange-yellow in Fig. 2) of streamlines is resulted. Only streamlines that propagate to the SN (shown in red in Fig. 2) appear in the result map (as orange-yellow voxels in Fig. 2). This

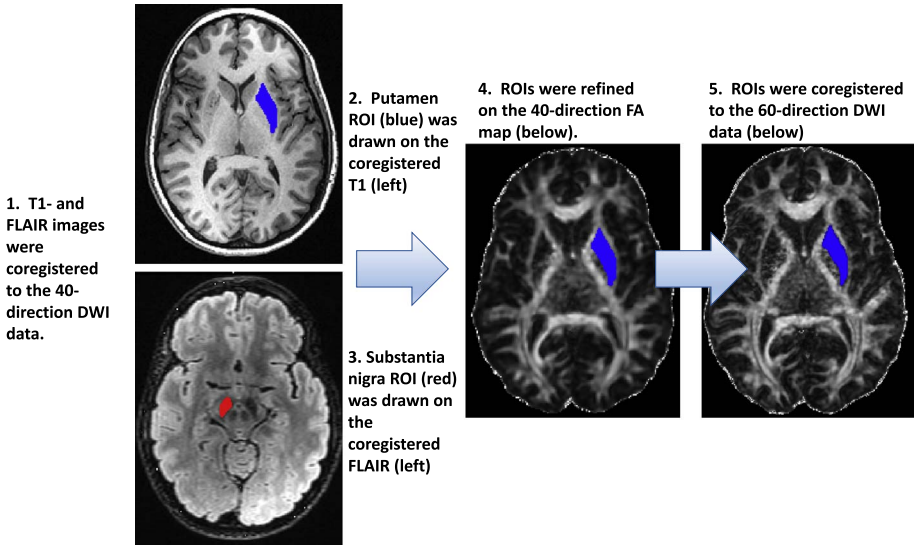

Fig. 1. Method for Defining Regions of Interest (ROIs). 1. High contrast structural images were coregistered to the 40-direction DWI data. 2. The putamen ROI (blue, upper left) was outlined on sequential T1-weighted axial images extending from top of lateral ventricles to the anterior commissure. 3. The substantia nigra (SN) ROI (red, lower left) was outlined on axial FLAIR images from the level of the red nucleus to superior cerebellar peduncle. 4. The putamen and SN ROIs were inspected and revised against the 40-direction FA maps (center). 5. Putamen and SN ROIs were coregistered to the 60-direction DWI data (right) and visually inspected against the 60-direction FA map.

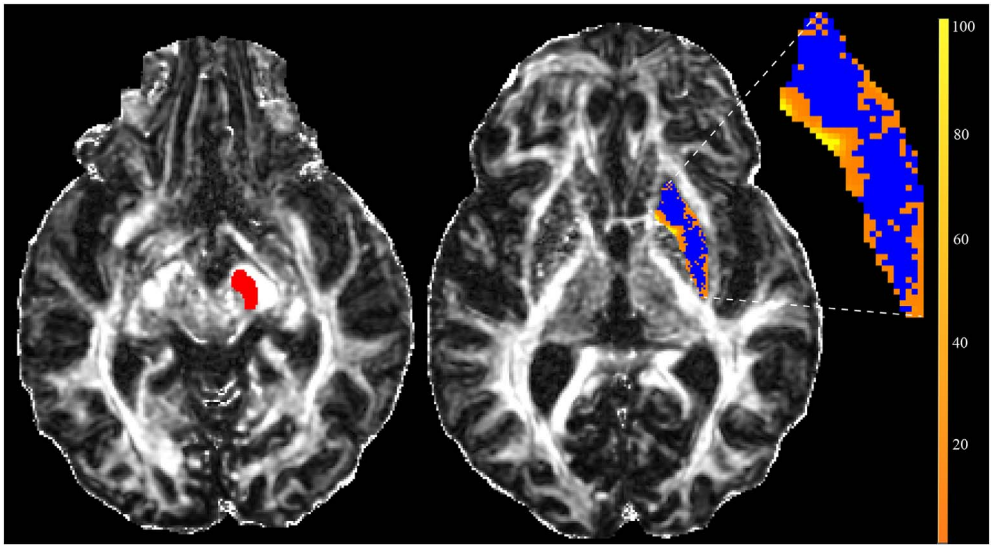

Fig. 2. Probabilistic Tractography in a Parkinson's subject.
A substantia nigra (SN) target region (red) and result map (blue/orange) from the probabilistic tracking approach are shown superimposed on the 60-direction FA map. The inset at right shows the magnified result map, in which blue areas represent voxels in the seed ROI (putamen) that do not generate streamlines and thus have values of zero. Values of the yellow-orange voxels (color scale at right) represent the number of seeding events (of 5000 trials) that reach the SN.

map does not quantify how strong a connection is; rather, it provides information about how robust a fiber tract is against the noise/uncertainty, and as such, is best thought of as confidence bounds on the location of the most likely connection (Behrens et al., 2003a). From the result map and putamen ROI, we extracted two variables, an index of connection probability (mean number of streamlines per voxel sampled = sum of voxel values in the result map/number of voxels in the putamen seed mask), and an index of streamline density (percentage of seeded voxels that generated streamlines = number of non-zero voxels in the result map/number of voxels in the seed mask × 100). For the purpose of statistical analyses, connection probability and streamline density, as well as the ROI-derived covariates (mean FA and MD within the ROIs as well as ROI volume) were organized as ipsilateral or contralateral to initial motor symptoms in PD patients, or averaged across hemispheres in controls.

2.2.5. Statistical analyses

Statistical analyses were conducted in SPSS (22.0, IBM, Chicago). Bivariate (Pearson) correlations were initially used to explore the relationship between age, gender, education, ROI-derived, and tractography variables. Generalized linear models were then constructed to evaluate our specific hypothesis that structural connectivity would be lower in PD, regardless of the contributions of potentially important covariates. These GLM's evaluated the effect of diagnostic group (PD or control) on putamen-SN connectivity with covariates of age, sex, and years of education. Volume of the seed mask (voxel number), as well as DWI values within the seed and target masks, were included as covariates when significantly correlated with the tractography outputs. Findings with a P value of < 0.05 were considered significant.

3. Results

Demographic and disease characteristics of the participants are summarized in Table 1. These data are summarized for all subjects (all of whom had 40-direction DWI data), as well as for the subgroup of subjects who had 60-direction DWI data of sufficient quality for analysis. The PD and control groups did not differ by age or gender, although the PD group was less well educated than the control group. PD patients, as expected, had higher (worse) functional scores on the Unified Parkinson's Disease Rating Scale (UPDRS). Of the PD group, all but 4 participants were taking anti-Parkinson medications (dopamine agonists, levodopa, amantadine, and/or monoamine oxidase inhibitors) at the time of study enrollment.

There was no difference between PD and control groups in the volume of the manually-defined seed (putamen) and target (SN) ROIs. A comparison of mean FA and MD values within the ROIs (Table 2) did not reveal consistent differences between disease groups. When considering the 40-direction data, PD patients had higher mean FA in the contralateral SN ($P = 0.02$), a trend towards higher FA in the ipsilateral SN ($P = 0.07$), and higher mean MD in the ipsilateral SN ($P = 0.02$). There were no significant differences in ROI FA or MD values derived from the 60-direction data.

Mean connection probability values were moderately correlated ($r = 0.31–0.36$, $P < 0.05$) with the seed mask (putamen) volume, but not with the target mask (SN) volume for both 40- and 60-direction data. Within the 40-direction data, mean connection probability was moderately correlated with putamen FA ($r = 0.22–0.26$, $P < 0.05$), and streamline density was moderately correlated with SN FA ($r = -0.22$ to -0.31, $P < 0.05$). Within the 60-direction data, mean connection probability was not correlated with either FA nor MD values within the ROI's, but the streamline density was correlated with putamen FA ($r = -0.49$ to -0.52, $P < 0.001$). Therefore, volume of the putamen seed mask, as well as SN and putamen FA, were included as covariates in GLMs constructed to evaluate the effect of group (PD versus control) on the tractography outputs.

A summary of the GLM results is shown in Table 3. We found a

Table 1
Characteristics of study participants.

Variable	PD	Control	P value
40-Direction DTI data			
Number of subjects (n)	40	44	
Age (y)	65.3 (9.6)	67.1 (8.1)	0.37
Gender (M:F)	32:8	32:12	0.44
Education (y)	15.8 (2.7)	17.2 (2.7)	0.02*
Disease duration (y)	6.0 (4.0)	n/a	n/a
UPDRS part 3 score	20.0 (9.7)	1.5 (1.6)	0.00*
PD symptom onset (R:L: symmetrical)	24:12:4	n/a	n/a
60-Direction DTI data			
Number of subjects	36	42	
Age (y))	64.5 (9.5)	66.8 (8.1)	0.25
Gender (M:F)	28:8	31:11	0.69
Education (y)	16.0 (2.6)	17.3 (2.7)	0.04*
Disease duration (y)	6.1 (4.2)	n/a	n/a
UPDRS part 3 score	20.3 (10.1)	1.6 (1.7)	0.00*
Side of onset (R:L: neither)	21:12:3	n/a	n/a

Mean values are displayed with standard deviations (SD) in parentheses. Abbreviations: PD = Parkinson's disease; n/a = not applicable; y = years.
* $P < 0.05$ for unpaired *t*-test between PD and control.

Table 2
Seed and target ROI characteristics.

	PD Ipsi.	PD Contra.	Control L/R average	P-value	
				Ipsi.	Contra.
40-Direction DWI data					
Volume (voxels)					
Putamen	1878 (368)	1865 (370)	1853 (350)	0.75	0.88
SN	381 (104)	392 (110)	371 (86)	0.63	0.33
FA					
Putamen	0.209 (0.020)	0.210 (0.023)	0.205(0.023)	0.35	0.31
SN	0.546 (0.052)	0.551 (0.049)	0.528 (0.035)	0.07	0.02*
MD					
Putamen	0.00081 (0.00009)	0.00080 (0.00009)	0.00079 (0.00005)	0.22	0.88
SN	0.00078 (0.00006)	0.00077 (0.00006)	0.00075 (0.00003)	0.02*	0.31
60-Direction DWI data					
Volume (voxels)					
Putamen	5424 (1051)	5355 (1056)	5320 (1024)	0.66	0.89
SN	1050 (304)	1085 (312)	1035 (234)	0.80	0.41
FA					
Putamen	0.265 (0.038)	0.264 (0.031)	0.256 (0.032)	0.26	0.24
SN	0.591 (0.077)	0.602 (0.070)	0.600 (0.058)	0.56	0.89
Mean diffusivity					
Putamen	0.00067 (0.00005)	0.00067 (0.00006)	0.00067 (0.00003)	0.37	0.52
SN	0.00072 (0.00022)	0.00070 (0.00017)	0.00067 (0.00010)	0.23	0.38

Mean values are displayed with standard deviations in parentheses. Abbreviations: Contra. = contralateral to symptom onset; Ipsi. = ipsilateral to symptom onset; L = left; PD = Parkinson's disease; SD = standard deviation; R = right; ROI = region of interest.
* $P < 0.05$ for unpaired *t*-test between PD and control means.

significant effect of group (PD < Control, P = 0.006) on mean connection probability for the brain hemisphere contralateral to initial symptoms in the 60-direction data. There was also an effect of group (PD < Control) on the streamline density in both brain hemispheres and both DWI datasets (40-direction, $P < 0.01$; 60-direction, $P \leq 0.001$). The 60-direction data provided a better separation between PD and control means. Although the 95% confidence intervals were distinct between groups (Fig. 3), there was overlap of individual streamline density values. Inclusion of ROI volumes and FA values as covariates in the models did not significantly alter the degree of significance for the group effect. Within 60-direction PD data, there was a trend towards lower connection probability (P = 0.146) in the brain hemisphere contralateral to symptom onset, where pathology is expected to be more extensive than on the ipsilateral side. We did not find convincing relationships between connection probability measures and age, gender, or education in the combined dataset, nor with disease severity measures (UPDRS III scores, disease duration) in the PD group.

4. Discussion

This hypothesis-driven investigation used probabilistic tractography to generate putamen to SN connectivity estimates from diffusion-weighted data in 40 PD patients and 44 control subjects; it is one of a few similar investigations to date. The main finding was that estimates of anatomical connectivity were on average lower in PD patients than healthy controls, potentially reflecting reduced brainstem white matter microstructural integrity. Since tractography results are critically dependent on how ROIs are defined (size, location, and extension into white matter tracks, which typically generate much higher connection probabilities than gray matter), we were careful to systematically define ROIs using both structural and diffusion images, to use ROIs whose average size did not differ by disease group or brain hemisphere, and to control for ROI size and diffusion characteristics in our statistical analyses. To further develop the technique, we compared results from a 40-direction DWI sequence to an optimized 60-direction sequence. For the 60-direction dataset, slices were overlapped, which does yield a tradeoff between sampling (better), resolution (slightly worse), spatial sampling (better), and SNR (better). While we have not exhaustively compared the effects of this type of sampling, we did expect the SNR boost is a worthy tradeoff for more coarse spatial resolution with finer spatial sampling. The most promising measure obtained from these data was an index of streamline density, the mean value of which was significantly lower in PD in both brain hemispheres and both diffusion sequences. The 60-direction sequence was more sensitive to putative disease-related differences, producing a greater separation between PD and control means. This may in part be because the more information contained in diffusion data, the lower the uncertainty in estimates of the principal diffusion direction (Behrens et al., 2003a).

Using various tractography approaches, previous studies (Menke et al., 2009; Tan et al., 2015; Zhang et al., 2015) have reported either reduced connection probability or altered diffusion measures within the nigrostriatal pathway. However, the only probabilistic tractography study of similar size to the one reported here (Sharman et al., 2013), found no significant difference in SN-putamen connectivity in PD. Three additional studies that used deterministic tracking found reduced FA and increased mean and radial (RD) diffusivity along the pathway (Tan et al., 2015; Zhang et al., 2015). Tan et al. found the PD subjects to have a lower streamline count that was correlated with UPDRS scores.

In the present study, we observed significantly lower mean striatonigral streamline density in PD; however, scatter plots of the data (Fig. 3) showed overlap in values between disease groups that will limit its use as a diagnostic measure. Nonetheless, with future improvements in diffusion-based techniques, it is possible that this measure may prove

Table 3
Tractography results.

	40-Direction diffusion data			60-Direction diffusion data		
	Control mean(SD)	PD mean(SD)	Std. Beta/P	Control mean(SD)	PD mean(SD)	Std. Beta/P
Connection probability[a]						
Ipsilateral	65.7(40)	59.4(60)	− 0.053/0.564	76.5(49)	60.8(45)	− 0.140/0.139
Contralateral	65.7(40)	58.06(49)	− 0.063/0.425	76.5(49)	48.0(43)	− 0.260/0.006*
Streamline density[b]						
Ipsilateral	87.0 (7.9)	81.2 (12.2)	− 0.242/0.008*	72.0(13.7)	58.6(14.9)	− 0.367/0.000028*
Contralateral	87.0 (7.9)	81.4 (11.7)	− 0.217/0.009*	72.0(13.7)	61.0(14.7)	− 0.286/0.001*

Abbreviations: SD, standard deviation; PD, Parkinson's disease; Std., standardized.
[a] Mean number of samples that generate streamlines that reach the SN per seeded putamen voxel.
[b] Percentage of voxels in the putamen that generate one or more streamlines that reach the SN.
* GLM yields $P < 0.05$ for the main effect of group.

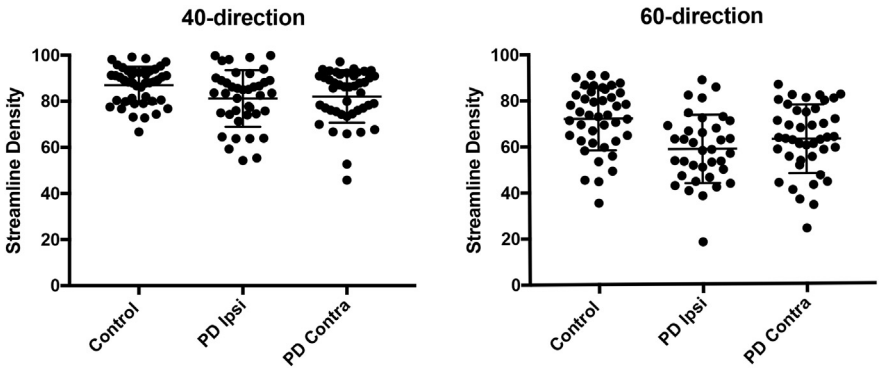

Fig. 3. Streamline density measures from 40- and 60- direction DWI data.
The distribution of the streamline density index for controls (averaged across brain hemispheres) in comparison to PD for brain hemispheres ipsilateral (Ipsi) and contralateral (Contra) to initial motor symptoms. Horizontal bars indicate the mean and SD for each distribution. Although means were significantly different between disease groups (40-direction $P < 0.01$; 60-direction $P \leq 001$), there was overlap of individual values.

useful for tracking longitudinal changes within individuals.

A number of studies (Menke et al., 2009; Vaillancourt et al., 2009; Schwarz et al., 2013; Lenfeldt et al., 2015, and others) have investigated diffusion measures within the SN as a potential biomarker for PD. Some studies have reported reduced FA in the dorsal SN (Vaillancourt et al., 2009), while subsequent studies have reported no consistent FA difference when averaging across the entire structure (Schwarz et al., 2013), as was observed in the present study. A recent meta-analysis suggested that high between-study variance in SN FA limits it's value as a diagnostic biomarker (Schwarz et al., 2013). A recent longitudinal study (Loane et al., 2016) found that although baseline SN DWI values did not differ between PD and control groups, the PD group had lower FA and higher MD at 18-month follow-up in comparison to the control baseline. This study suggests that diffusion measures within the SN may prove useful for tracking disease progression.

5. Limitations

Several limitations should be mentioned. Although the PD and control groups were age- and gender-matched, there was a difference in years of formal education that was controlled for by entering these covariates into the regression models. Further, the cross-sectional design cannot control for individual differences in baseline measures as well as can be done in a longitudinal study. From a technical standpoint, the striatonigal pathway is a non-dominant connection compared to local projection fibers such as the corticospinal tract and thus is difficult to isolate using tractography. Further, the use of gray matter regions as seeds, in which there is high local uncertainty in fiber orientation, may bias towards producing streamlines emanating from more superficial voxels.

6. Conclusions

In spite of the significant difference in mean putamen-SN streamline density between PD and control groups, the overlap in individual values precludes the use of this measure as a disease classifier. Improvement in the separation between means by the 60- in comparison to between the 40-direction data suggests that technical improvements are possible. Further refinements in the technique, including the use of high contrast structural images to define sub regions of the SN, improvements in diffusion signal acquisition and modeling, and longitudinal studies, may eventually produce results of clinical value.

Role of the funding source

This work was supported by Merit Review Award 101CX000555 from the United States Department of Veterans Affairs Clinical Sciences Research and Development. Funding for the acquisition of pilot data for technique development was provided by the University of Wisconsin Institution for Clinical and Translational Research (ICTR) award number 1UL1RR025011. The authors would also like to acknowledge the support provided by the University of Wisconsin Alzheimer's Disease Research Center Clinical Core for subject recruitment and the Neuroimaging Core for study design and data analysis and as well facilities and resources at the Geriatric Research, Education, and Clinical Center (GRECC) of the William S. Middleton Memorial Veterans Hospital, Madison, WI. The content is solely the responsibility of the authors and does not represent the official views of the US Department of Veteran Affairs, nor the US Government, nor the National Institutes of Health. Importantly, the authors wish to thank our volunteers, without whom this work would not be possible.

Conflict of interest

The authors declare no conflicts of interest.

Funding source

Department of Veterans Affairs, Clinical Sciences R&D Merit Review Award Number 101CX000555, ICTR/NIH Award Number 1UL1RR025011.

References

Behrens, T.E., Johansen-Berg, H., Woolrich, M.W., Smith, S.M., Wheeler-Kingshott, C.A., Boulby, P.A., Barker, G.J., Sillery, E.L., Sheehan, K., Ciccarelli, O., Thompson, A.J., Brady, J.M., Matthews, P.M., 2003a. Non-invasive mapping of connections between human thalamus and cortex using diffusion imaging. Nat. Neurosci. 6, 750–757.

Behrens, T.E., Woolrich, M.W., Jenkinson, M., Johansen-Berg, H., Nunes, R.G., Clare, S., Matthews, P.M., Brady, J.M., Smith, S.M., 2003b. Characterization and propagation of uncertainty in diffusion-weighted MR imaging. Magn. Reson. Med. 50, 1077–1088.

Behrens, T.E., Berg, H.J., Jbabdi, S., Rushworth, M.F., Woolrich, M.W., 2007. Probabilistic diffusion tractography with multiple fibre orientations: what can we gain? NeuroImage 34, 144–155.

Braak, H., Del Tredici, K., Rub, U., de Vos, R.A., Jansen Steur, E.N., Braak, E., 2003. Staging of brain pathology related to sporadic Parkinson's disease. Neurobiol. Aging 24, 197–211.

Fahn, S., Elton, R.L., 1987. UPDRS Development Committee. The Unified Parkinson's Disease Rating Scale. In: Fahn, S., Marsden, C.D., Calne, D.B., Goldstein, M. (Eds.), Recent Developments in Parkinson's Disease, 2nd edn. Macmillan Healthcare Information, Florham Park, NJ, pp. 153–163 (293–304).

Folstein, M.F., Folstein, S.E., McHugh, P.R., 1975. “Mini-mental state”. A practical method for grading the cognitive state of patients for the clinician. J. Psychiatr. Res. 12, 189–198.

Freed, C.R., Greene, P.E., Breeze, R.E., Tsai, W.Y., DuMouchel, W., Kao, R., Dillon, S., Winfield, H., Culver, S., Trojanowski, J.Q., Eidelberg, D., Fahn, S., 2001. Transplantation of embryonic dopamine neurons for severe Parkinson's disease. N. Engl. J. Med. 344, 710–719.

Goren, B., Kahveci, N., Eyigor, O., Alkan, T., Korfali, E., Ozluk, K., 2005. Effects of intranigral vs intrastriatal fetal mesencephalic neural grafts on motor behavior disorders in a rat Parkinson model. Surg. Neurol. 64 (Suppl. 2), S33–41.

Greve, D.N., Fischl, B., 2009. Accurate and robust brain image alignment using boundary-based registration. NeuroImage 48, 63–72.

Hughes, A.J., Daniel, S.E., Kilford, L., Lees, A.J., 1992. Accuracy of the clinical diagnosis of idiopathic Parkinson's disease: a clinico-pathologic study of 100 cases. J. Neurol. Neurosurg. Psychiatry 55, 181–184.

Jenkinson, M., Smith, S., 2001. A global optimisation method for robust affine registration of brain images. Med. Image Anal. 5, 143–156.

Jenkinson, M., Bannister, P., Brady, M., Smith, S., 2002. Improved optimization for the

robust and accurate linear registration and motion correction of brain images. NeuroImage 17, 825–841.
Jenkinson, M., Beckmann, C.F., Behrens, T.E., Woolrich, M.W., Smith, S.M., 2012. Fsl. NeuroImage 62, 782–790.
Karimi, M., Tian, L., Brown, C.A., Flores, H.P., Loftin, S.K., Videen, T.O., Moerlein, S.M., Perlmutter, J.S., 2013. Validation of nigrostriatal positron emission tomography measures: critical limits. Ann. Neurol. 73, 390–396.
Lenfeldt, N., Larsson, A., Nyberg, L., Birgander, R., Forsgren, L., 2015. Fractional anisotropy in the substantia nigra in Parkinson's disease: a complex picture. Eur. J. Neurol. 22, 1408–1414.
Loane, C., Politis, M., Kefalopoulou, Z., Valle-Guzman, N., Paul, G., Widner, H., Foltynie, T., Barker, R.A., Piccini, P., 2016. Aberrant nigral diffusion in Parkinson's disease: a longitudinal diffusion tensor imaging study. Mov. Disord. 31, 1020–1026.
Lucking, C.B., Durr, A., Bonifati, V., Vaughan, J., De Michele, G., Gasser, T., Harhangi, B.S., Meco, G., Denefle, P., Wood, N.W., Agid, Y., Brice, A., French Parkinson's Disease Genetics Study, G, European Consortium on Genetic Susceptibility in Parkinson's, D, 2000. Association between early-onset Parkinson's disease and mutations in the Parkin gene. N. Engl. J. Med. 342, 1560–1567.
Ly, M., Adluru, N., Destiche, D.J., Lu, S.Y., Oh, J.M., Hoscheidt, S.M., Alexander, A.L., Okonkwo, O.C., Rowley, H.A., Sager, M.A., Johnson, S.C., Bendlin, B.B., 2016. Fornix microstructure and memory performance is associated with altered neural connectivity during episodic recognition. J. Int. Neuropsychol. Soc. 22, 191–204.
Menke, R.A., Scholz, J., Miller, K.L., Deoni, S., Jbabdi, S., Matthews, P.M., Zarei, M., 2009. MRI characteristics of the substantia nigra in Parkinson's disease: a combined quantitative T1 and DTI study. NeuroImage 47, 435–441.
Moore, R.Y., Bloom, F.E., 1978. Central catecholamine neuron systems: anatomy and physiology of the dopamine systems. Annu. Rev. Neurosci. 1, 129–169.
Oguz, I., Farzinfar, M., Matsui, J., Budin, F., Liu, Z., Gerig, G., Johnson, H.J., Styner, M., 2014. DTIPrep: quality control of diffusion-weighted images. Front. Neuroinform. 8, 4.
Palfi, S., Leventhal, L., Chu, Y., Ma, S.Y., Emborg, M., Bakay, R., Deglon, N., Hantraye, P., Aebischer, P., Kordower, J.H., 2002. Lentivirally delivered glial cell line-derived neurotrophic factor increases the number of striatal dopaminergic neurons in primate models of nigrostriatal degeneration. J. Neurosci. 22, 4942–4954.
Parent, A., 1990. Extrinsic connections of the basal ganglia. Trends Neurosci. 13, 254–258.
Schwarz, S.T., Abaei, M., Gontu, V., Morgan, P.S., Bajaj, N., Auer, D.P., 2013. 2013. Diffusion tensor imaging of nigral degeneration in Parkinson's disease: a region-of-interest and voxel-based study at 3T and systematic review with meta-analysis. Neuroimage Clin. 3, 481–488.
Sharman, M., Valabregue, R., Perlbarg, V., Marrakchi-Kacem, L., Vidailhet, M., Benali, H., Brice, A., Lehericy, S., 2013. Parkinson's disease patients show reduced cortical-subcortical sensorimotor connectivity. Mov. Disord. 28, 447–454.
Smith, S.M., 2002. Fast robust automated brain extraction. Hum. Brain Mapp. 17, 143–155.
Tan, W.Q., Yeoh, C.S., Rumpel, H., Nadkarni, N., Lye, W.K., Tan, E.K., Chan, L.L., 2015. Deterministic tractography of the nigrostriatal-nigropallidal pathway in Parkinson's disease. Sci Rep 5, 17283.
Vaillancourt, D.E., Spraker, M.B., Prodoehl, J., Abraham, I., Corcos, D.M., Zhou, X.J., Comella, C.L., Little, D.M., 2009. High-resolution diffusion tensor imaging in the substantia nigra of de novo Parkinson disease. Neurology 72, 1378–1384.
Zhang, Y., Wu, I.W., Buckley, S., Coffey, C.S., Foster, E., Mendick, S., Seibyl, J., Schuff, N., 2015. Diffusion tensor imaging of the nigrostriatal fibers in Parkinson's disease. Mov. Disord. 30, 1229–1236.